(2)

TECHNICAL REPORT BRL-TR-3289

BRL

DESIGN AND ANALYSIS OF KINETIC ENERGY PROJECTILES USING FINITE ELEMENT OPTIMIZATION

BRETT R. SORENSEN

NOVEMBER 1991

U.S. ARMY LABORATORY COMMAND

BALLISTIC RESEARCH LABORATORY
ABERDEEN PROVING GROUND, MARYLAND

NOTICES

Destroy this report when it is no longer needed. DO NOT return it to the originator.

Additional copies of this report may be obtained from the National Technical Information Service, U.S. Department of Commerce, 5285 Port Royal Road, Springfield, VA 22161.

The findings of this report are not to be construed as an official Department of the Army position, unless so designated by other authorized documents.

The use of trade names or manufacturers' names in this report does not constitute indorsement of any commercial product.

REPORT DOCUMENTATION PAGE

Form Approved
OMB No. 0704-0188

1. AGENCY USE ONLY (Leave blank)	2. REPORT DATE	3. REPORT TYPE AND DATES COVERED
	November 1991	Final, 1 Jan 90 - 1 Jul 90

4. TITLE AND SUBTITLE

Design and Analysis of Kinetic Energy Projectiles Using Finite Element Optimization

5. FUNDING NUMBERS

PR: 1L162618AH80

6. AUTHOR(S)

Brett R. Sorensen

7. PERFORMING ORGANIZATION NAME(S) AND ADDRESS(ES)

U.S. Army Ballistic Research Laboratory
ATTN: SLCBR-TB-P
Aberdeen Proving Ground, MD 21005-5066

8. PERFORMING ORGANIZATION REPORT NUMBER

9. SPONSORING/MONITORING AGENCY NAME(S) AND ADDRESS(ES)

U.S. Army Ballistic Research Laboratory
ATTN: SLCBR-DD-T
Aberdeen Proving Ground, MD 21005-5066

10. SPONSORING/MONITORING AGENCY REPORT NUMBER

BRL-TR-3289

11. SUPPLEMENTARY NOTES

12a. DISTRIBUTION/AVAILABILITY STATEMENT

Approved for public release; distribution is unlimited.

12b. DISTRIBUTION CODE

13. ABSTRACT *(Maximum 200 words)*

This report discusses the minimization of the parasitic mass of a 120-mm cannon launched kinetic energy projectile. The purpose of the study was to design a minimum mass aluminum sabot to launch both depleted uranium and tungsten heavy alloy penetrator materials for the M829 penetrator geometry. The minimization was conducted by implementing finite element techniques. A parametric model of a kinetic energy projectile using a double ramp traction sabot was constructed and an input stream for the ANSYS engineering analysis software was created. This input stream created the mesh for the projectile, solved for the stresses for each penetrator material, and implemented the optimization capabilities within ANSYS to minimize the mass of the sabot. Twenty-five iterations were required to reach a local minimum of the objective function (sabot mass) and resulted in a 15% decrease in sabot mass. The entire process (initial design and evaluation, optimization, and final analysis) was completed in one day (9 hours wall clock and 2 man-hours) on a personal workstation.

14. SUBJECT TERMS

kinetic energy projectiles; sabots; sabot design; finite element analysis; optimization

15. NUMBER OF PAGES

28

16. PRICE CODE

17. SECURITY CLASSIFICATION OF REPORT	18. SECURITY CLASSIFICATION OF THIS PAGE	19. SECURITY CLASSIFICATION OF ABSTRACT	20. LIMITATION OF ABSTRACT
UNCLASSIFIED	UNCLASSIFIED	UNCLASSIFIED	SAR

INTENTIONALLY LEFT BLANK.

TABLE OF CONTENTS

INTENTIONALLY LEFT BLANK.

LIST OF FIGURES

LIST OF TABLES

INTENTIONALLY LEFT BLANK.

1. BACKGROUND

As emerging technologies and materials advance tomorrow's heavy armor threat, the need to develop improved cannon-launched kinetic energy (KE) projectiles continues to be an important issue within the Army. Historically, as the armor protection levels have increased, penetrator aspect ratio (length-to-diameter), mass, and velocity have also increased. The current trends in modern antiarmor KE ammunition have been in high length-to-diameter ratio (L/D), fin-stabilized penetrators utilizing discarding sabots. An example of a fielded projectile, the M829, is depicted in Figure 1. Figure 1 presents an isometric view of the penetrator, three of four sabot petals, and associated hardware (windshield, fins, and obturator).

Figure 1. Isometric View of a KE Projectile Fired From a Tank Cannon.

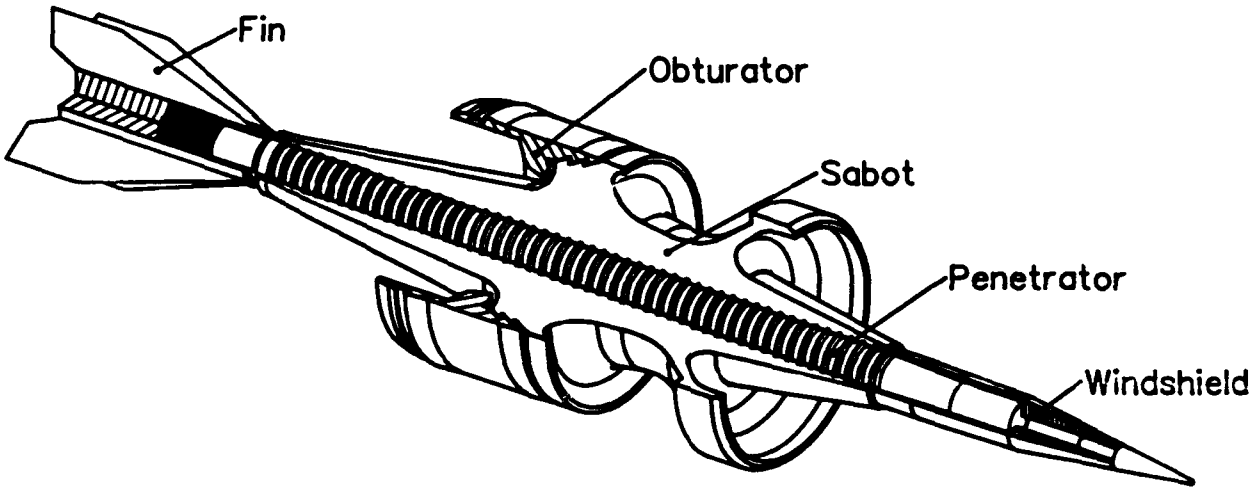

A long rod penetrator is essentially a right circular cylinder with an aspect ratio of 10 or larger and is made of a high density material. The geometry requirement of a cylinder is not absolute. Concessions are made to attach the windshield and fin, and more importantly, to provide an interface between the penetrator and the sabot. This interface transfers the pressure incident on the sabot to the penetrator. It consists of annular buttress grooves in the forward section of the penetrator/sabot interface and a friction drive (e.g., fine threads) in the aft section.

The sabot is made of aluminum (or some other low density material) and consists of three or four sections (petals). When the sabot is assembled around the penetrator, a one-piece plastic obturator is pressed onto the sabot. This provides a seal between the sabot and the cannon to prevent combustion products from leaking and also provides radial compression to hold the sabot on the penetrator prior to placing the projectile into the cannon.

The sequence of events for a launch is as follows. The propelling charge is ignited and begins to burn. Pressure inside the cannon builds rapidly as the projectile starts to move, accelerating the projectile along the length of the cannon toward the muzzle. Typical pressure, displacement, velocity, and acceleration histories experienced by a KE projectile are plotted in Figure 2. As the projectile exits the muzzle, the radial constraint of the cannon is removed and the high-pressure gases exiting the cannon cause the obturator to fracture (hoop failure). As the projectile enters the ambient atmosphere, aerodynamic forces on the sabot, along with affects from the gun gases, cause the sabot petals to separate and disengage from the penetrator. After the sabot discards, the lethal mechanism (penetrator, windshield, and fin) travels down range to the target.

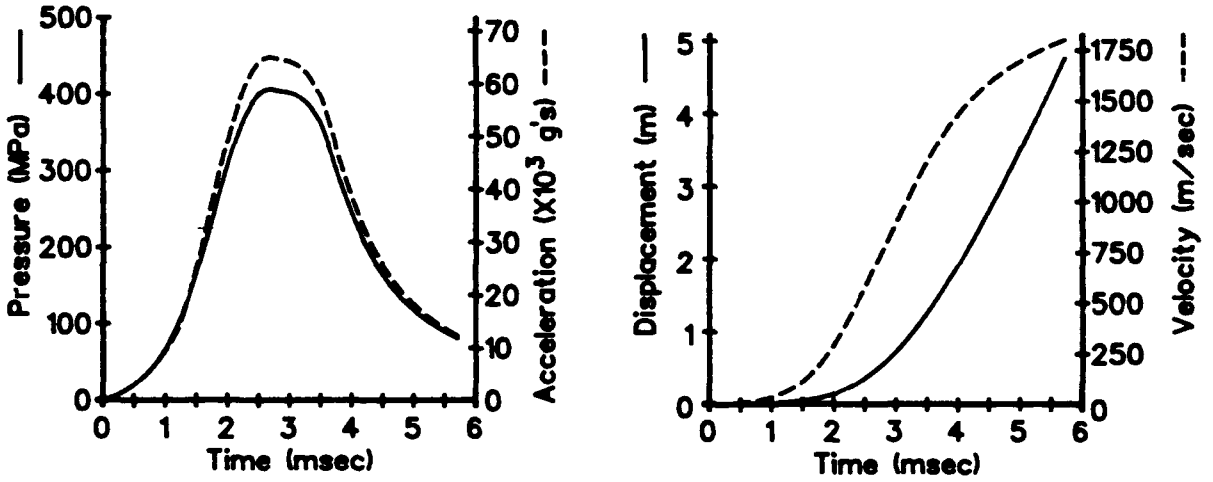

Figure 2. Pressure, Displacement, Velocity and Acceleration Curves for a KE Projectile.

An automated design technique has been developed to maintain structural integrity during the interior ballistic phase of launch. The Kinetic Energy Projectile Design Program, KEPDEP, is an interactive program implemented on a computer-aided design (CAD) network to generate projectile geometry and to interface with several finite element programs, including ANSYS

(Sorensen 1991; DeSalvo and Gorman 1987; PRISM/DDM User Manuals 1990; Hallquist 1983). Using finite element techniques, simplified models of the projectile can be implemented to insure that the in-bore stresses do not exceed the allowable material limits. KEPDEP is used to generate a complete mesh with boundary conditions, or a parameter list to be used in a parameterized optimization as will be discussed in this report.

2. INTRODUCTION

An experiment aimed at evaluating the terminal ballistic performance of two ballistic materials, depleted uranium (DU) and a tungsten heavy alloy (WHA), for a particular penetrator geometry posed a new design problem. It was decided that one sabot design would be utilized to launch both penetrator types; furthermore, due to the velocity requirements of the experiment, the sabot mass must be minimized. This created a problem because DU and WHA have different mechanical properties (Table 1). DU is alloyed with 0.75% of titanium by weight and is aged with a heat treatment; it has very good elongation properties and a nonlinear stress-strain behavior. The WHA used is 93% tungsten by weight and is produced by a liquid phase sintering process. The tungsten grains are in a tungsten-iron-nickel-cobalt matrix. The material is thermomechanically processed by swaging and then heat treated. The material is almost perfectly elastic-plastic, and due to low elongation and its microstructure, is prone to fracture. Considering the facts that DU is a nonlinear material while WHA is not, and the large difference in elastic moduli, obtaining a mass efficient sabot design would be difficult by manual means. Therefore, a parametric model of a KE projectile was devised to be used in an optimization study.

Table 1. Material Properties

Material	Elastic Modulus (GPa)	Density (kg/m^3)	Poisson's Ratio	Compressive Yield (MPa)	Tensile Yield (MPa)
DU	165	18,600	.22	931	862
WHA	338	17,600	.29	1,207	1,303
Al	69	2,800	.33	496	496

3. MODELING ASSUMPTIONS

Almost any finite element analysis makes some simplifying assumptions and several are made in this analysis. The primary assumptions are that the model is axisymmetric and quasi-static in nature (Drysdale 1981). The axisymmetry assumption can be used since the sabot is under radial compression, thus preventing the petals from sliding relative to each other. The quasi-static solution requires that the model be constrained in the axial direction and that force be conserved by applying an acceleration in the direction opposite that of the applied pressure. This assumption ignores any transverse loads, which is acceptable since the maximum axial load is at least an order of magnitude larger. Furthermore, although the rise time for the pressure is very short, dynamic analyses show that wave propagation is not significant. Therefore, the maximum dynamic loads can be replaced by quasi-static loads. Additional assumptions are made to simplify the geometry and can be seen in Figure 3. These geometry assumptions simplify the bulkhead, the bell and the penetrator/sabot interface. The interface is simplified by smearing the details into a homogenous material with shared nodes. The homogenous material properties are the same as the sabot material properties with the exception of using an average density. Also note the addition of lumped masses to represent the windshield and fin. Figure 3 also names the significant features of the penetrator and sabot to clarify future discussions.

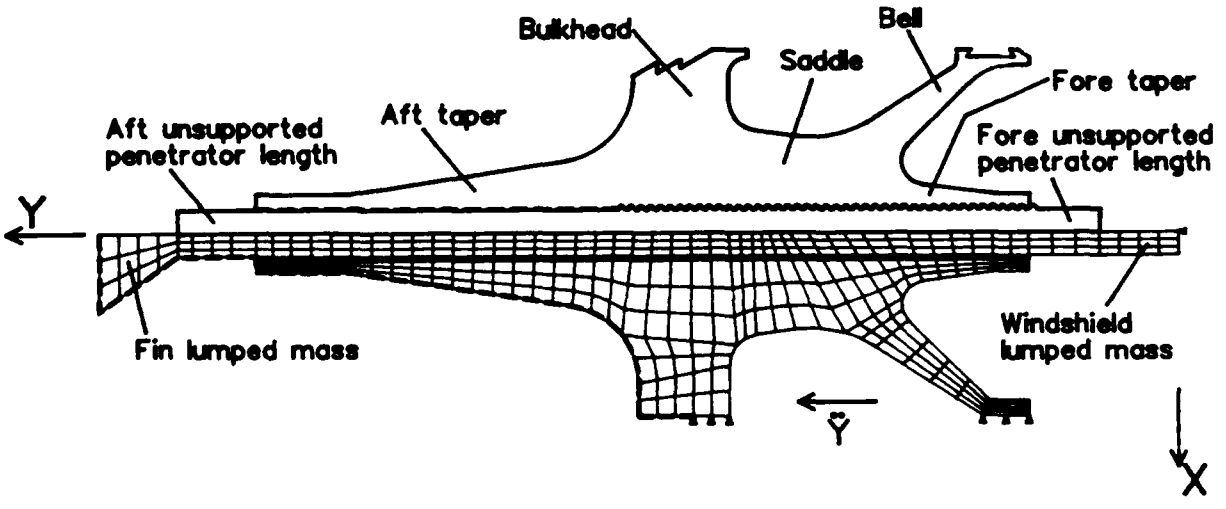

Figure 3. Axisymmetric Profile of a Penetrator and Sabot Designed by KEPDEP and the Finite Element Mesh Generated by ANSYS via the KEPDEP Interface.

The axisymmetry option in ANSYS predetermines the coordinate system. The four-node, quadrilateral element utilized requires that the y-axis be the axis of symmetry and suggests that all elements be in the first quadrant (+x, +y). Therefore, the +x direction is radial and the +y direction is axial. The origin is placed at the front of the windshield's lumped mass and the penetrator extends along the positive +y axis.

The maximum pressure due to the combustion of propellant occurs at the breech of the gun. Since the projectile and some of the propellant is accelerating, the pressure seen by the projectile, the base pressure, is less than the breech pressure. A force balance about the breech of the cannon at maximum pressure is seen in Equation 1 and is the result of the Lagrange correction (Department of the Army 1965),

$$P_c A_B = \left(M + \frac{1}{2} C \right) \ddot{z}, \tag{1}$$

where

P_C = Breech pressure (Pa)
A_B = Area of the cannon bore (m^2)
M = Projectile mass (kg)
C = Propellant mass (kg)
$\ddot{z}$ = Acceleration (m/s^2).

Summing the forces about the projectile leads to

$$P_B A_B = M \ddot{z}, \tag{2}$$

where

P_B = *Base pressure* (Pa).

Reorganizing Equations 1 and 2, the base pressure is determined as

$$P_B = \frac{P_C}{1 + \frac{1}{2} \frac{C}{M}}. \tag{3}$$

To obtain the quasi-static solution, the node at the origin is assumed to be stress free and is constrained in the y direction. The base pressure, computed by Equation 3, is applied on the free edges of the model which are behind the bulkhead. To balance the force introduced by the base pressure, the acceleration computed by Equation 2 must be applied in the -y direction. The model is very sensitive to the balance of the base pressure and axial acceleration, and due to numerical inaccuracies, the computed acceleration may induce a stress at the axially constrained node. This can be checked in the post-processor by examining the axial stress component at this node. If the magnitude of the stress is greater than 0.5% of the maximum stress in the model, the acceleration is modified accordingly to bring this stress level to acceptable limits, thus balancing the forces at the constrained node.

An additional static pressure exists within the model. As the projectile is forced into the cannon, the obturator is radially compressed to provide a seal for the propellant gasses. This exerts a pressure on the bulkhead since the obturator material is relatively incompressible. Therefore, a 140 MPa pressure is placed on the aft portion of the bulkhead. The last boundary conditions applied are to constrain the remaining nodes along the sabot/cannon interface. In reality, this is a sliding contact where the projectile can move radially inward, but since the projectile is experiencing radial expansion in these areas, using a radial constraint is accurate. The boundary conditions are shown on the nodal presented in Figure 4.

4. PARAMETRIC MODEL

The projectile profile displayed in Figure 3 will be adapted to a parametric model. To create the model, 25 geometric parameters, 10 material parameters, and 3 cannon parameters are required. A list of these parameters with a short description is presented in Table 2 and a sketch of the parameterized model is provided in Figure 4. A brief discussion on generating the model will be presented

The mesh generation capability of the ANSYS preprocessor will be implemented to create the nodes and elements; therefore, the model is divided into quadrilateral areas to define the geometry. All necessary keypoints and line segments are defined first. (The keypoints and line segments are required to define the quadrilateral areas.) The areas are created and meshed using a different element type for each material type. The constraints are set and the

Table 2. KE Projectile Parameters

GEOMETRIC PARAMETERS

XR	Penetrator radius.	YR	Penetrator length.
YF	Fore unsupported penetrator length.	XF1	Forward flat radius of the sabot.
YFF1	Length of the forward flat.	MF1	Slope of the forward taper.
XF2	Starting radius of the saddle.	YFF2	Starting location of the saddle.
MF2	Slope of the saddle.	YB	Beginning of the bell.
DB	Initial thickness of the bell.	MB1	Slope of the front of the bell.
DMB	Difference in slope between bell surfaces.	YO	Beginning of the bulkhead.
DO	Thickness of the bulkhead.	YA	Aft unsupported penetrator length.
XA	Aft flat radius of the sabot.	YAF	Length of the aft flat.
MA	Slope of the aft taper.	R1	Forward blend radius of the bell.
R2	Aft blend radius of the bell.	R3	Forward blend radius of the bulkhead.
R4	Aft blend radius of the bulkhead.	WWS	Windshield mass.
WFN	Fin mass.		

MATERIAL PROPERTIES

PE	Young's modulus of the penetrator.	PRO	Penetrator density.
PNU	Poisson's ratio of the penetrator.	PCOM	Compressive yield of the penetrator.
PTEN	Tensile yield of the penetrator.	SRO	Young's modulus of the sabot.
SRO	Sabot density.	SNU	Poisson's ratio of the sabot.
SCOM	Compressive yield of the sabot.	STEN	Tensile yield of the sabot.

CANNON PARAMETERS

XB	Gun bore radius	PC	Chamber pressure.
CM	Charge mass.		

Prefix definitions:

- X - Radial variable
- Y - Axial variable
- D - Delta distance
- M - Slope
- S - Sabot material property
- P - Penetrator material property
- R - Fillet (blend) radius

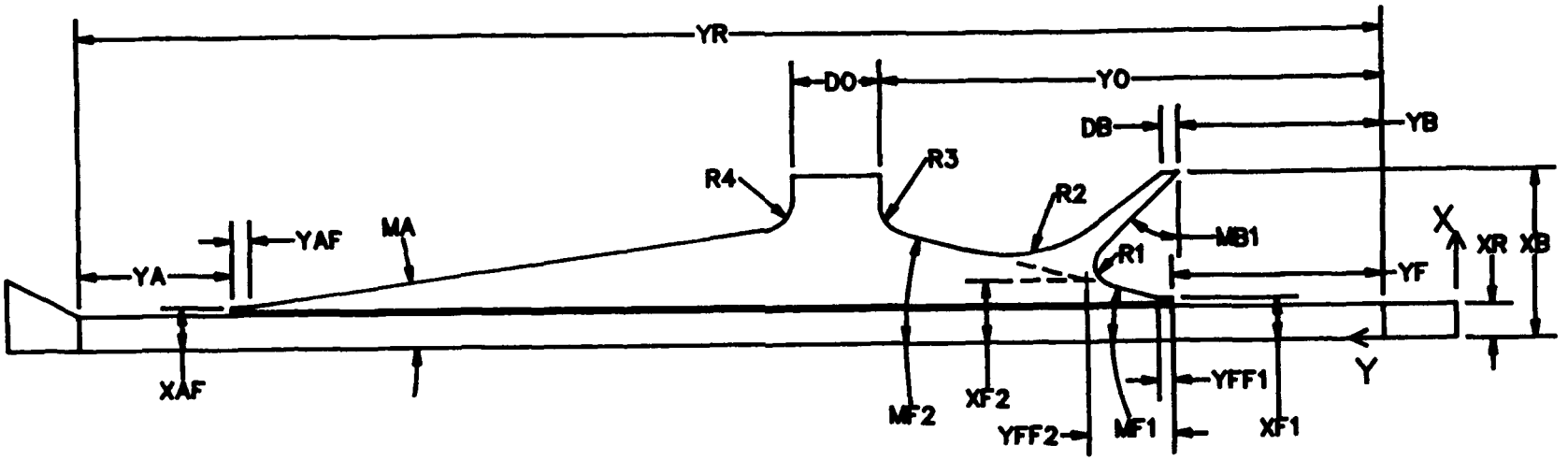

a) Projectile Dimensioned With Associated Parameters.

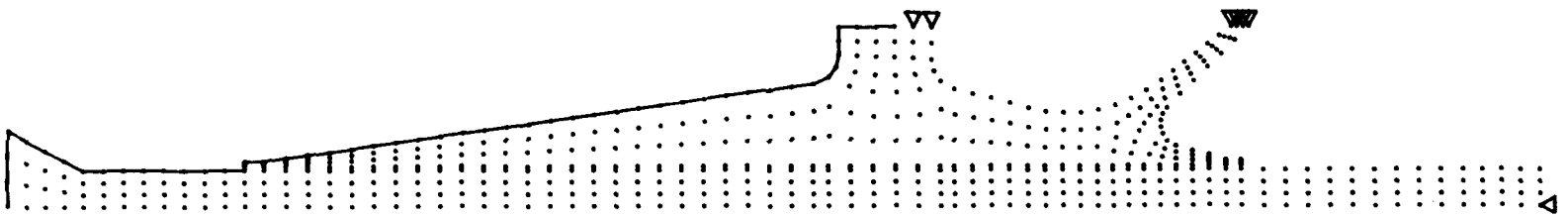

b) Nodal Plot With Boundary Conditions.

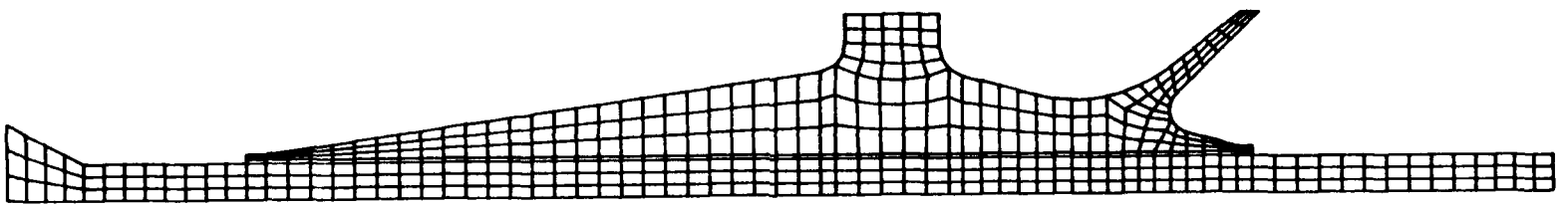

c) Element Plot.

Figure 4. Parametric Model of a KE Projectile and the Resulting Finite Element Mesh.

pressure on the bulkhead from the obturator being radially compressed is applied. The remaining boundary conditions, base pressure and acceleration, cannot be set until the projectile mass is known because they are functions of the mass. A solution input deck is written and executed. By entering the ANSYS post-processor, the volumes for each element type can be obtained. Multiplying each resulting volume by the appropriate density and summing, the projectile mass can be determined. The objective function, sabot mass, is also defined at this point. Reentering the preprocessor, the remaining boundary conditions are calculated and set, thus completing the model.

5. DESIGN PROCESS

5.1 Initial Design. Before the optimization process could begin, an initial design was required. For the purpose of this report, penetrator geometry from an existing projectile, the M829, was used. The goal was to design a minimum weight sabot to launch both DU and WHA penetrators. To assist the optimization process, the initial projectile design should be feasible as specified by the state variables. This is not a requirement for the process to work, but if the design parameters are too far from the acceptable design space, a feasible solution may not be obtained.

The process for obtaining the initial design was as follows. The penetrator design was known and the initial sabot design is to be provided by KEPDEP. Based on prior design experience with both materials, WHA was chosen as the initial material. After the sabot design was obtained, a finite element analysis was completed for each penetrator material. If post-processing revealed that the sabot design was feasible for both penetrator materials, an initial configuration had been obtained. If not, the sabot was modified and the analysis process repeated until a feasible design was reached. At this point, a parameter file defining the geometry (Table 2) was generated by KEPDEP.

5.2 Optimization. The ANSYS optimization module uses three different types of variables: design, state, and objective. The design variables are the parameters which are allowed to change from iteration to iteration. These variables are drawn from the pool of parameters which specify the finite element model which are listed in Table 2. For each iteration, a unique set of design variables will exist to provide a new finite element model each time. The

objective variable is the parameter which is being minimized, in this case, sabot mass. The state variables define the optimization function over which the objective variable is minimized. State variables can be almost any retrievable data from the finite element analysis, but in this example, they are stresses from specified regions of the finite element mesh. Both design and state variables are provided operating ranges. For the design variables, this range specifies the acceptable values which can be used during the optimization. The state variable ranges specify whether each state variable is acceptable for any given iteration and provide the rules governing the objective function.

At this point, the user must decide which of the parameters that define the sabot are to be used as design variables in the optimization process. Acceptable ranges for the design variables must also be determined. Furthermore, if any additional state variables are desired, they must also be defined. After all these decisions are made, the input deck in the Appendix must be modified appropriately and the analysis can begin. A flow chart of this process is presented in Figure 5.

In this analysis, the sabot details which remained constant were the locations of the sabot ends, and the geometry of the bell and bulkhead. The features which were allowed to change and their associated parameters are: the fore taper (XF1, YFF1, MF1), the saddle (XF2, YFF2, MF2); the aft taper (XA, YAF, MA), and the locations of the bell (YB) and bulkhead (YO). These 11 parameters were assigned design variable status. In addition to the 11 design variables, R1 and R2 were also allowed to change to prevent an error in geometry creation from occuring. That is to say, if the design variables for a particular iteration had values such that a particular blend radius could not be placed between the specified lines, R1 and R2 would be changed to accommodate the design variable set to prevent premature termination. This is not an advisable solution, but is deemed better than program termination. If either of these radii are modified, a flag is set to inform the designer to inspect the printed output and optimization parameters for any unacceptable affects. The best solution is to insure beforehand that the ranges on the design variables will not allow the creation of faulty geometry. This was the case for the analysis presented in this report.

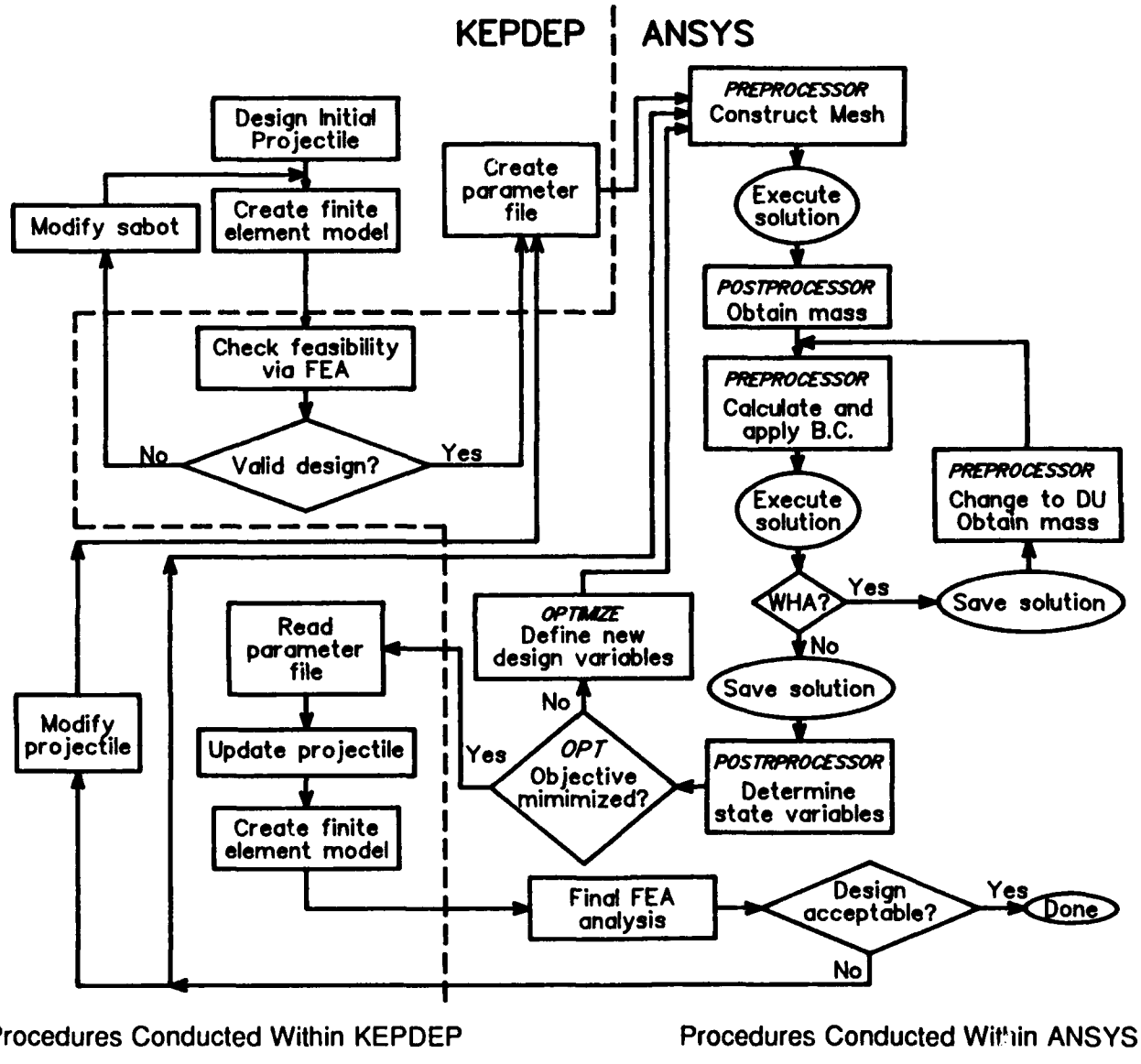

Figure 5. Flow Chart of the Design Logic Beginning With the Initial Design and Progressing Through the Optimization and Final Analysis.

Six state variables were used in the optimization and are all yield limits of the various materials in the analysis. The state variables are the maximum axial compressive stress in the penetrator, the maximum effective tensile stress in the penetrator, and the maximum effective stress in the sabot (excluding stress concentrations) for each penetrator material. The limits are determined by the yield criteria for each material and the maximum stress level acceptable.

6. RESULTS

Execution of the input deck (see Appendix) resulted in a local minimum for the objective variable in 25 iterations. Of these 25 iterations, 14 were feasible and 5 resulted in values for the objective variable which are within 2% of the minimum. Iterations were judged infeasible if any state variable exceeded its limits. The mass of the sabot was reduced by 15% from 3.06 kg for initial design to 2.60 kg for the "best" solution. Numerical simulations of the combustion process were performed using a standard propellant and a maximum breech pressure of 655 MPa (Anderson and Ficke 1987). This operating pressure is the same as used in the analysis and is 93% of the 120-mm cannon's maximum rating. This analysis provided an accurate estimate for maximum loading conditions and the muzzle velocity. Using the initial and the "best" designs, the calculations showed a 2.9% increase in muzzle velocity, from 1,769 m/s to 1,820 m/s. For the "best" design, the projectile experienced a maximum base pressure of 403 MPa and an acceleration of 65,700 g's.

The finite element mesh used within the optimization process consisted of approximately 450 nodes and 350 elements with 900 active degrees of freedom. The material properties of the lump masses and WHA penetrator were linear (elastic), where as the remaining materials were nonlinear (elastic-plastic). The initial solution passes, used to determine the projectile mass and boundary conditions, were performed with linear material properties to minimize the number of iterations required. The final solution pass for each penetrator material was performed with the nonlinear materials active to obtain an accurate stress state. The optimization analysis was executed on an APOLLO DN4500 as a background process in 7.25 hours.

In Figure 6, the objective variable and state variables are plotted against iteration number for the optimization process. In each of the plots, feasible solutions are defined by circles and the state variable limits are denoted by broken lines. Additionally, state variables for DU and WHA are labeled. The objective variable (sabot mass) is presented in Figure 6a, and the state variables of sabot stress, compressive penetrator stress, and effective tensile penetrator stress are in Figures 6b, 6c, and 6d, respectively. The first impression of these curves is the oscillatory nature with a large magnitude early in the optimization process. Somewhere between iterations 10 and 15, the curves dampen considerable, with the exception of the compressive penetrator stresses for WHA. The large oscillations suddenly dampening is explained by the number of design variables. In order to sufficiently describe the design surface (objective function), at least one iteration per variable is required. To minimize the complexity of the input stream, these initial iterations are randomly generated by the optimization routine. Once the surface is constructed, the optimization routine can select the design variables for subsequent iterations much better and the state variables fluxuate less. Examination of the state variables show that all three DU state variables are at the design limits whereas the WHA state variables for the feasible designs are generally five percent below their limits. Therefore, the three DU state variables were the dominating factors in the analysis.

The design variables for the "best" sabot design were utilized to construct the final projectile design. After completing this design, a final analysis was conducted using this sabot with both penetrator materials. The resulting penetrator stresses are presented in Figure 7 with the WHA results in Figure 7a and the DU results in 7b. The stress profiles presented represent the axial and the effective stresses along the penetrator centerline (solid lines) and the minor diameter (dashed lines). The state variable limits for the penetrator materials are presented as the horizontal phantom lines and are also labeled. Several points can be made about this figure. Examination of the stresses at the penetrator's diameter reveals two sharp discontinuities. These discontinuities occur at each end of the sabot and can be used to define each of the unsupported penetrator lengths and the length of the sabot. Furthermore, these features can be used to define the penetrator stress at each unsupported length. Figure 7b shows that the stress limits for the DU penetrator are slightly exceeded, this is due to the tolerance placed on the state variables. In the aft section of the penetrator, the elevated stress level will have minimal effect since the overstressed state does not exist

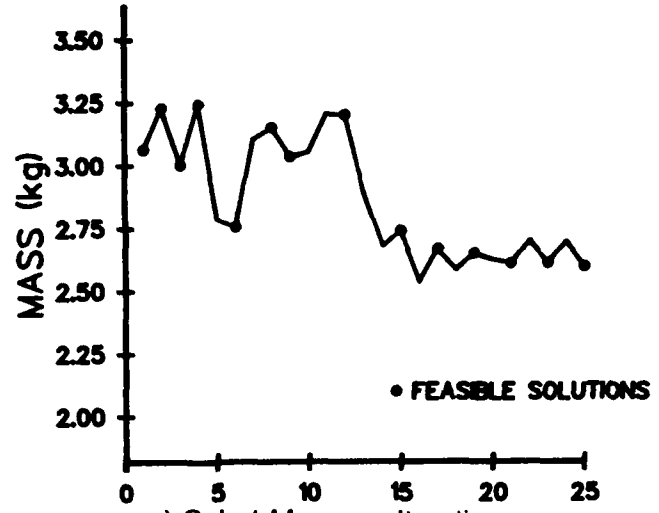

a) Sabot Mass vs. Iteration

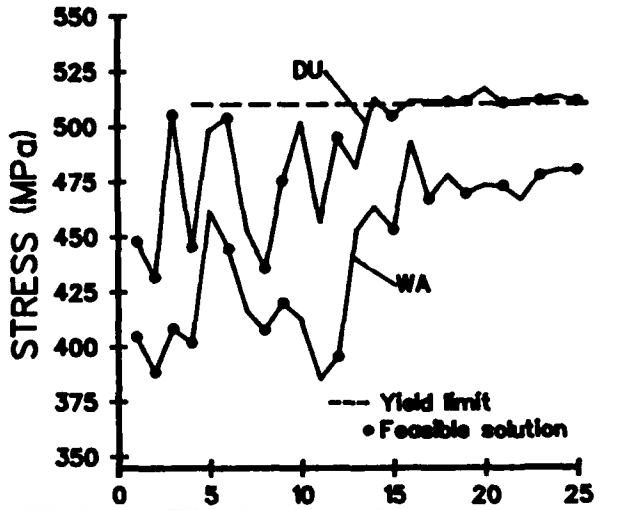

b) Maximum Effective Sabot Stress vs. Iteration

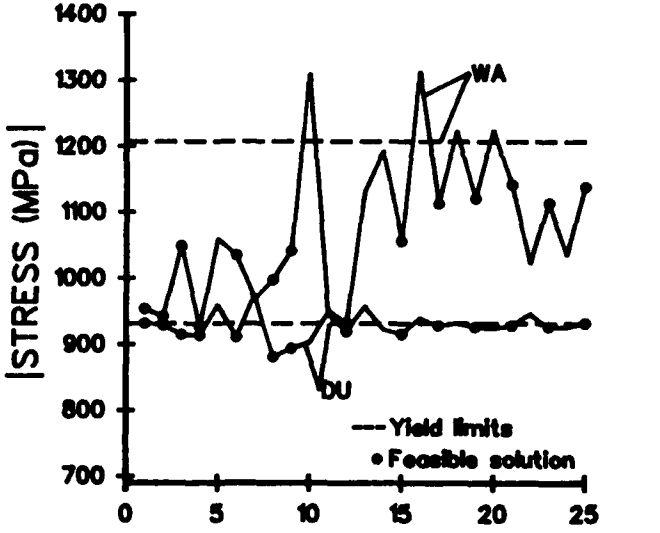

c) Maximum Penetrator Compressive Stress vs. Iteration

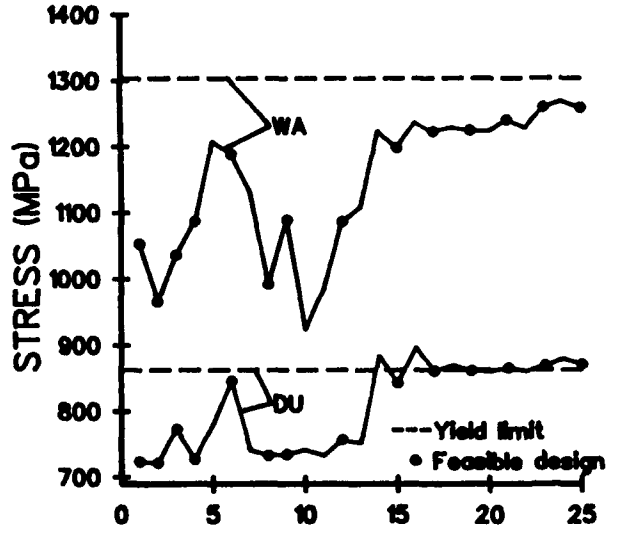

d) Maximum Penetrator Effective Tensile Stress vs. Iteration

Figure 6. Results of the Objective and State Variables From the Optimization Process.

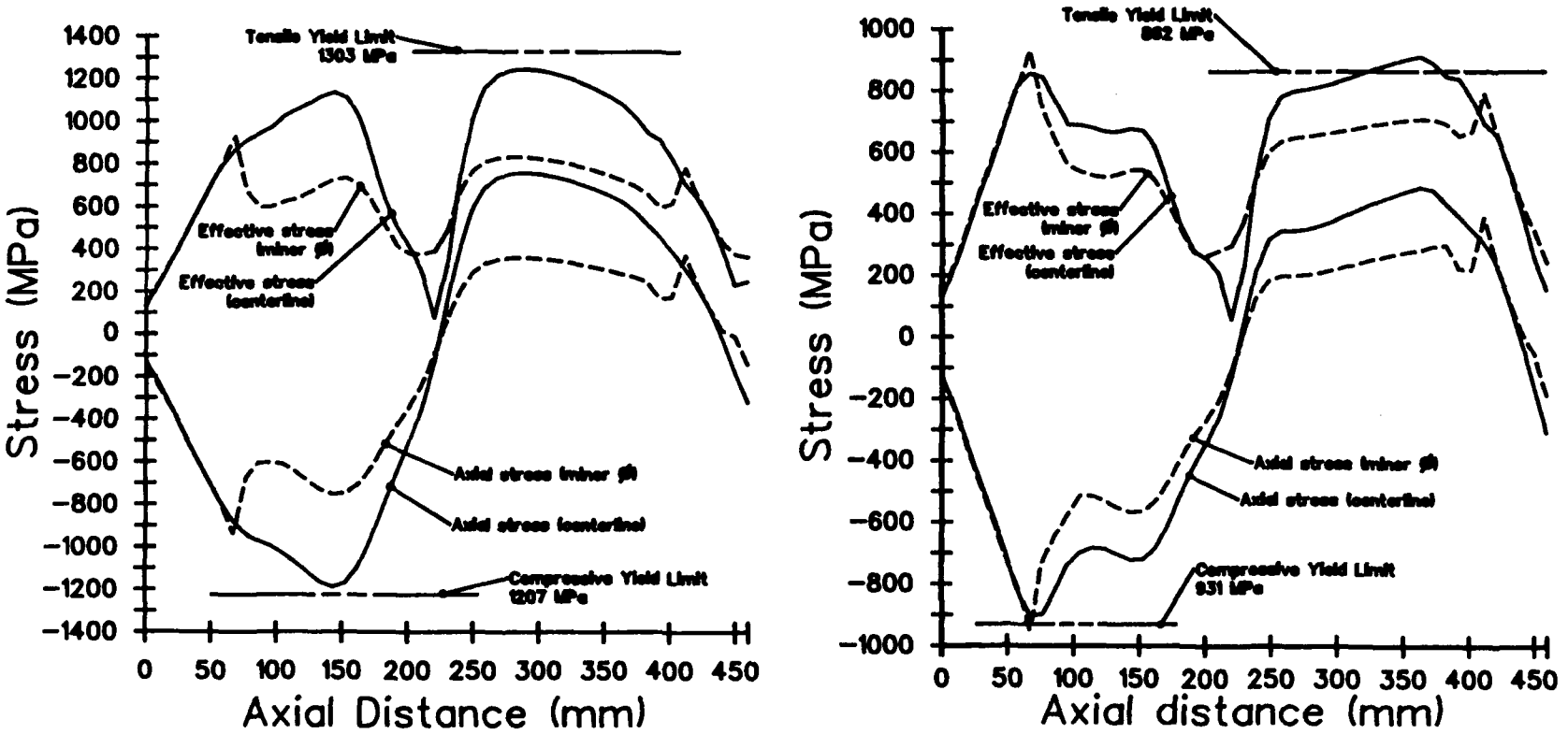

a) Final Results for the WHA Penetrator

b) Final Results for the DU Penetrator

Figure 7. Results for the Final Analysis for Each Penetrator Material Using the "Best" Sabot.

throughout the crosssection. Furthermore, since DU has excellent ductility and an ultimate tensile stress exceeding 1,275 MPa, this slight overstressed condition is acceptable. However, the stress at the forward, unsupported length should be examined more carefully because the stress state exceeds the design limit through the entire cross section and buckling could be a concern. Buckling, or yielding of the WHA penetrator is not a concern because the maximum stresses in the penetrator and sabot are 5% below their respective yield limits.

The decision to use the M829 penetrator to document this design procedure had a significant drawback. Due to the aspect ratio and length of the penetrator, the differences between the penetrator materials did not have a significant affect on the design process. In this case, the sabot could have been designed for the DU penetrator alone and resulted in nearly the same design. However, if a penetrator with increased length or aspect ratio were used in the analysis, the result would most likely be different. As penetrator length increases, the modulus mismatch between the WHA penetrator and the sabot will result in the compressive stresses in the portion of the penetrator under the sabot saddle to become the determining factor. But in the aft portion of the penetrator, and throughout the sabot, the DU projectile will still be the driving influence. When this happens, the analysis is much more complex and design optimization will be the most beneficial.

7. CONCLUSIONS

The implementation of parameterization and optimization techniques within ANSYS were extremely helpful in solving the complex and difficult design problem presented in this report. The parametric analysis and design language proved to be quite adept in creating a finite element mesh for complex geometry. By using KEPDEP to provide an initial design and ANSYS to minimize the sabot mass, an attractive result was produced with one day's effort. Attempting a problem of this type without the methods discussed here could take days or even weeks; therefore, a substantial decrease in design time was realized, leading to increased productivity. Furthermore, since the optimization process was run in a background environment, the actual commitment in time was less than two hours. One hour or less was required to generate the initial design and set the design and state variables and another hour to perform the final detailed analysis and review all results.

8. REFERENCES

Anderson, R. D., and K. D. Ficke. "IBHVG2 -- A User's Guide." BRL TR-2829, U.S. Army Ballistic Research Laboratory, Aberdeen Proving Ground, Aberdeen, MD, July 1987.

Department of the Army. Engineering Design Handbook: Interior Ballistics of Guns. AMC Pamphlet 706-150, Washington, DC, February 1965.

DeSalvo, G. J., and R. W. Gorman. ANSYS Engineering Analysis Systems User's Manual, Vol. I and II (Rev. 4.3), Swanson Analysis Systems Inc., Houston, PA, June 1987.

Drysdale, W. H. "Design of Kinetic Energy Projectiles for Structural Integrity." BRL-TR-02365, U.S. Army Ballistic Research Laboratory, Aberdeen Proving Ground, MD, September 1981.

Hallquist, J. O. "MAZE - An Input Generator for DYNA2D and NIKE2D." LLNL Report UCID 19029, Rev. 2, Lawrence Livermore National Laboratory, Livermore, CA, June 1983.

Hallquist, J. O. "NIKE2D - A Vectorized Implicit, Finite Deformation Finite Element Code for Analyzing the Static and Dynamic Response of 2-D Solids with Interactive Rezoning and Graphics." LLNL Report UCID 19677m, Rev. 1, Lawrence Livermore National Laboratory, Livermore, CA, December 1986.

PRISM/DDM User's Manuals. CALMA, A Division of Prime Computer, Inc., San Diego, CA, (~1990).

Sorensen, B. R. "Implementation of a CAD/CAM System to Design, Analyze, and Manufacture Prototype Kinetic Energy Projectiles." BRL-TR-3272, U.S. Army Ballistic Research Laboratory, Aberdeen Proving Ground, MD, September 1991.

INTENTIONALLY LEFT BLANK.

APPENDIX:

PARTIAL LISTING OF THE ANSYS INPUT DECK

INTENTIONALLY LEFT BLANK.

A partial listing of the ANSYS (Revision 4.3A) input deck used in the preceding analysis is presented. Most of the file has been omitted to maintain confidentiality. The following variables are defined: v1, ..., v5, are the volumes of each element type; d1, ..., d5 are the densities for each element type; yacc, yac1, yac2 are axial acceleration values; sy01, sy02 are axial stresses at the constrained node; mt and ms are the projectile and sabot masses; the remaining variables are self-explanatory.

```
/com, Read initial parameter file
*use,parm.opt
/com, Set initial values and constants
/prep7
/title,Sabot optimization

/com, Set materials for tungsten projectile
/com, Linear material for tungsten
/com, Non-linear for grooves and sabot
                .
                .
                .
/com, Construct geometry and mesh
                .
                .
                .
/com, Set switches for one iteration solution
knl,0
iter,1
afwr
fini

/com, Execute solution
/exe
/input,27
fini
```

```
/com, Use post-processing to determine projectile
/com, and sabot masses.
/com, calculate pressure and acceleration.
/post1
stress,volu
set,1
ersel,type,1
nelem
ssum
*get,v1,ssum,volu
nall$eall
ersel,type,2
nelem
ssum
*get,v2,ssum,volu
nall$eall
ersel,type,3
nelem
ssum
*get,v3,ssum,volu
nall$eall
ersel,type,4
nelem
ssum
*get,v4,ssum,volu
nall$eall
```

```
ersel,type,5
nelem
ssum
*get,v5,ssum,volu
nall$eall
mt=(((v1*d1)+(v2*d2))+((v3*d3)+(v4*d4)))+(v5*d5)
ms=(v3*d3)
pb=pc/(1+(cm/(2*mt)))
zac1=(pb*ab)/mt
zac2=zac1+100
fini
/prep7
resume
*use,parm.ans
/com, Add boundary conditions at R=XB
nrsel,x,xb
nrsel,y,,((yo1+yo2)/2)+1
d,all,ux,0
nall
nrsel,x,xb
nrsel,y,((yo1+yo2)/2)+1,yo2+1
psf,all,,,20000
nall
/com, Add base pressure and two accelerations
lsrsel,,13,21
nline,1
psf,all,,,pb
nall
acel,,-zacc
lwri
acel,,-zac1
lwri
afwr
fini
```

```
/com, Execute solution for two load steps
/exe
/input,27
fini

/com, Post-process and interpolate the <hrt>
/com, acceleration to minimize the
/com, axial stress and the windshield
/post1
set,1
nrsel,y,
nrsel,x
nsort,sy
*get,sy01,max
nall
set,2
nrsel,y,
nrsel,x
nsort,sy
*get,sy02,max
nall
xt=(zac1-zac2)/(sy01-sy02)
zacc=(-xt*sy02)+zac2
fini

/com, Enter PREP7 and apply accurate <hrt>
/com, acceleration.  Use three load steps to <hrt>
/com, minimize the plasticity ratio.
/com, Set switches for multiple iterations
/prep7
resume
*use,parm.ans
knl,1
iter,-20
```

```
cnvr,.1
lsrsel,,13,21
nline,1
psf,all,,,pb*.5
nall
acel,,-zacc*.5
lwri
nline,1
psf,all,,,pb*.8
nall
acel,,-zacc*.8
lwri
nline,1
psf,all,,,pb
nall
acel,,-zacc
lwri
afwr
fini

/com, Solve for the tungsten projectile stresses
/exe
/input,27
fini

/com, Save the tungsten solution
/copy,12,31

/prep7
resume
*use,parm.ans
/com, Change to uranium material properties
.
.
.
```

```
/com, Compute new projectile mass and B.C.s
mt0=mt
mt=(((v1*d1)+(v2*d2))+((v3*d3)+(v4*d4)))+(v5*d5)
pb=pc/(1+(cm/(2*mt)))
zacc=zacc*mt0/mt
nline,1
psf,all,,,pb*.5
nall
acel,,-zacc*.5
lwri
nline,1
psf,all,,,pb*.8
nall
acel,,-zacc*.8
lwri
nline,1
psf,all,,,pb
nall
acel,,-zacc
lwri
afwr
fini

/com, Solve for the uranium projectile stresses
/exe
/input,27
fini

/com, Save the uranium solution
/copy,12,32

/com, Post-process to obtain state variables
/post1
```

```
nfile,31
set,3
/com, Tungsten state variables
                .
                .
                .
nfile,32
set,3
/com, Uranium state variables
                .
                .
                .
finish

/com, Optimization routine
/opt
/com, Objective variable
opvar,ms,obj,,,.001

/com, State variables for tungsten
opvar,scy1,sv,cmpw,0
opvar,ste1,sv,0,tenw
opvar,sse1,sv,0,ssbw
/com, State variables for uranium
opvar,scy2,sv,cmpd,0
opvar,ste2,sv,0,tend
opvar,sse2,sv,0,ssbd

/com, Design variables
opvar,yff1,dv, . . .
opvar,xf1,dv, . . .
opvar,mf1,dv, . . .
opvar,yff2, . . .
opvar,xf2,dv, . . .
opvar,mf2,dv, . . .
opvar,ma,dv, . . .
opvar,yaf,dv, . . .
opvar,xa,dv, . . .
opvar,yo1,dv, . . .
opvar,yb1,dv, . . .

opcopy
oprun,100,,,,30
oplist,all,,0
finish
```

No. of Copies	Organization
2	Administrator Defense Technical Info Center ATTN: DTIC-DDA Cameron Station Alexandria, VA 22304-6145
1	Commander U.S. Army Materiel Command ATTN: AMCAM 5001 Eisenhower Avenue Alexandria, VA 22333-0001
1	Commander U.S. Army Laboratory Command ATTN: AMSLC-DL 2800 Powder Mill Road Adelphi, MD 20783-1145
2	Commander U.S. Army Armament Research, Development, and Engineering Center ATTN: SMCAR-IMI-I Picatinny Arsenal, NJ 07806-5000
2	Commander U.S. Army Armament Research, Development, and Engineering Center ATTN: SMCAR-TDC Picatinny Arsenal, NJ 07806-5000
1	Director Benet Weapons Laboratory U.S. Army Armament Research, Development, and Engineering Center ATTN: SMCAR-CCB-TL Watervliet, NY 12189-4050
(Unclass. only)1	Commander U.S. Army Armament, Munitions and Chemical Command ATTN: AMSMC-IMF-L Rock Island, IL 61299-5000
1	Director U.S. Army Aviation Research and Technology Activity ATTN: SAVRT-R (Library) M/S 219-3 Ames Research Center Moffett Field, CA 94035-1000

No. of Copies	Organization
1	Commander U.S. Army Missile Command ATTN: AMSMI-RD-CS-R (DOC) Redstone Arsenal, AL 35898-5010
1	Commander U.S. Army Tank-Automotive Command ATTN: ASQNC-TAC-DIT (Technical Information Center) Warren, MI 48397-5000
1	Director U.S. Army TRADOC Analysis Command ATTN: ATRC-WSR White Sands Missile Range, NM 88002-5502
1	Commandant U.S. Army Field Artillery School ATTN: ATSF-CSI Ft. Sill, OK 73503-5000
(Class. only)1	Commandant U.S. Army Infantry School ATTN: ATSH-CD (Security Mgr.) Fort Benning, GA 31905-5660
(Unclass. only)1	Commandant U.S. Army Infantry School ATTN: ATSH-CD-CSO-OR Fort Benning, GA 31905-5660
1	Air Force Armament Laboratory ATTN: WL/MNOI Eglin AFB, FL 32542-5000
	Aberdeen Proving Ground
2	Dir, USAMSAA ATTN: AMXSY-D AMXSY-MP, H. Cohen
1	Cdr, USATECOM ATTN: AMSTE-TC
3	Cdr, CRDEC, AMCCOM ATTN: SMCCR-RSP-A SMCCR-MU SMCCR-MSI
1	Dir, VLAMO ATTN: AMSLC-VL-D
10	Dir, BRL ATTN: SLCBR-DD-T

No. of
Copies Organization

5 Director
Benet Weapons Laboratory
U.S. Army Armament Research,
Development, and Engineering Center
ATTN: SMCAR-CCB,
J. Keane
T. Allen
J. Vasilankis
J. Zweig
L. Johnson
Watervliet, NY 12189

7 Commander
U.S. Army Armament Research,
Development, and Engineering Center
ATTN: SMCAR-CCH-T,
S. Musalli
P. Christian
K. Fehsal
SMCAR-CCH-V, E. Fennell
SMCAR-CCH, J. DeLorenzo
SMCAR-CC,
R. Price
J. Hedderich
Picatinny Arsenal, NJ 07806-5000

2 Commander
U.S. Army Armament Research,
Development, and Engineering Center
ATTN: SMCAR-TD,
M. V. Lindner
T. Davidson
Picatinny Arsenal, NJ 07806-5000

1 Commander
Production Base Modernization Agency
U.S. Army Armament Research,
Development, and Engineering Center
ATTN: AMSMC-PBM-K
Picatinny Arsenal, NJ 07806-5000

3 PEO-Armaments
Project Manager
Tank Main Armament Systems
ATTN: SFAE-AR-TMA, COL Hartline
SFAE-AR-TMA-MD, C. Kimker
SFAE-AR-TMA-ME, K. Russell
Picatinny Arsenal, NJ 07806-5000

No. of
Copies Organization

2 Director
Lawrence Livermore National Laboratory
ATTN: R. Christensen
S. deTeresa
P.O. Box 808
Livermore, CA 94550

2 Pacific Northwest Lab
A Div of Battelle Memorial Inst.
Technical Information Section
ATTN: M. Smith
M. Garnich
P.O. Box 999
Richland, WA 99352

4 Director
Sandia National Laboratories
Applied Mechanics Department,
Division-8241
ATTN: C. W. Robinson
G. A. Benedetti
K. Perano
W. Kawahara
P.O. Box 969
Livermore, CA 94550-0096

1 Director
Los Alamos National Laboratory
ATTN: D. Rabern
WX-4 Division, Mail Stop G-787
P.O. Box 1633
Los Alamos, NM 87545

1 Olin Corporation
Flinchbaugh Division
ATTN: E. Steiner
P.O. Box 127
Red Lion, PA 17356

1 Olin Corporation
ATTN: L. Whitmore
10101 9th Street North
St. Petersburg, FL 33702

2 Alliant Techsystems, Inc.
ATTN: C. Candland
K. Ward
5640 Smetana Drive
Minnetonka, MN 55343

No. of Copies	Organization
2	Chamberlain Manufacturing Corp. Waterloo Facility ATTN: T. Lynch 550 Ester Street P.O. Box 2335 Waterloo, IA 50704

INTENTIONALLY LEFT BLANK.

USER EVALUATION SHEET/CHANGE OF ADDRESS

This laboratory undertakes a continuing effort to improve the quality of the reports it publishes. Your comments/answers below will aid us in our efforts.

1. Does this report satisfy a need? (Comment on purpose, related project, or other area of interest for which the report will be used.) _____

2. How, specifically, is the report being used? (Information source, design data, procedure, source of ideas, etc.) _____

3. Has the information in this report led to any quantitative savings as far as man-hours or dollars saved, operating costs avoided, or efficiencies achieved, etc? If so, please elaborate. _____

4. General Comments. What do you think should be changed to improve future reports? (Indicate changes to organization, technical content, format, etc.) _____

BRL Report Number BRL-TR-3289 Division Symbol _____

Check here if desire to be removed from distribution list. ____

Check here for address change. ____

Current address: Organization _____
Address _____

DEPARTMENT OF THE ARMY
Director
U.S. Army Ballistic Research Laboratory
ATTN: SLCBR-DD-T
Aberdeen Proving Ground, MD 21005-5066

OFFICIAL BUSINESS

BUSINESS REPLY MAIL
FIRST CLASS PERMIT No 0001, APG, MD

Postage will be paid by addressee.

Director
U.S. Army Ballistic Research Laboratory
ATTN: SLCBR-DD-T
Aberdeen Proving Ground, MD 21005-5066

NO POSTAGE NECESSARY IF MAILED IN THE UNITED STATES